Experimental observation of very low-frequency macroscopic modes in a dusty plasma

G. Praburam[a] and J. Goree[b]
Department of Physics and Astronomy, The University of Iowa, Iowa City, Iowa 52242

(Received 28 July 1995; accepted 16 January 1996)

Images of a cloud of grains in a dusty plasma reveal a pair of very low-frequency modes, termed here the filamentary and great void modes. The plasma was a radio-frequency discharge formed between parallel-plate graphite electrodes. A cloud of 100 nm carbon particles was produced by accretion of carbon atoms produced by sputtering the graphite. The cloud was illuminated with a laser sheet and imaged with a video camera. The great void mode was a spoke-shaped region of the cloud that was free of dust and rotated azimuthally in the discharge. The filamentary mode had the appearance of turbulent striations, with a smaller amplitude than the great void. The filamentary mode sometimes appeared as a distinctive vortex, curling in the poloidal direction. Both modes had a very low frequency, on the order of 10 Hz. Two possible causes of the modes are discussed. The low phase velocity of the modes may be consistent with a dust-acoustic wave. Alternatively, the great void may be an ionization wave that moved the dust about, since a modulation in the glow was seen moving at the same speed as the void. It is argued that existing theories of waves in dusty plasmas assume weakly collisional plasmas, which may be unsuitable for explaining experimental results in laboratory dusty plasmas, since they are often strongly coupled. [S1070-664X(96)02204-5]

I. INTRODUCTION

A dusty plasma is an ionized gas containing solid grains, which become charged by collecting electrons and ions.[1] The dust grains represent another species in the plasma, with a larger mass and charge than the ions, but a much lower charge-to-mass ratio. The grain's charge Q_d is proportional to its radius and to the electron temperature.[2] In laboratory experiments where electron emission is negligible, Q_d is negative, because electrons have a higher thermal velocity than ions. The grains usually have a kinetic temperature near room temperature, since they are in contact with neutral gas, although superthermal velocities have been observed in some experiments.[3,4] Like the electrons and ions, charged dust grains exhibit collective behavior. One manifestation of this is a Coulomb lattice, which has been reported in several recent experiments.[5–11] Another is wave phenomena. In this paper we report an experimental observation of unstable modes and turbulent waves in a dusty plasma.

To date, only a few laboratory experiments with dusty plasmas have been reported where waves or modes were detected. Chu and I[7] reported very low-frequency ($\approx$12 Hz) modes with a wavelength of about 0.5 cm, which they detected in the motion of their strongly coupled charged grains. They used a radio-frequency discharge, with a vertical dc electric field that suspended the particles in the sheath region immediately above a horizontal electrode. Based on the apparent phase velocity of 6 cm/s in that experiment, D'Angelo[12] has suggested that the fluctuations were a dust-acoustic mode, although his analysis does not explicitly account for the strong coupling that was present in the experiment. A similar interpretation was made by Barkan *et al.*,[13] who used a video camera to record planar wave fronts of a polydisperse kaolin dust cloud. The oscillating mode they observed had a large amplitude, a 15 Hz frequency and a 0.6 cm wavelength. Nitrogen was added to their potassium Q-machine plasma, and a current was drawn parallel to a magnetic field to produce a discharge with an electric field that levitated the grains.

Predating these experiments, theorists predicted the existence of a dust-acoustic wave. This mode can be described as a sound wave with compression and rarefaction of the dust cloud.[11,14,15] Theoretical dispersion relations for a variety of other modes in dusty plasmas have been reported as well.[16] Most of these were developed using the two-fluid model or other formalisms that are appropriate for a weakly collisional plasma, but not for a strongly coupled plasma. Waves and instabilities occur in strongly coupled plasmas, just as they do in ordinary liquids and solids. However, there is no reason to expect them to obey dispersion relations and damping rates derived for a weakly collisional plasma.

Dust grains tend to be strongly coupled in laboratory experiments because they have a large charge Q_d and a low-temperature T_d. This results in a large value of the Coulomb-coupling parameter,

$$\Gamma = Q_d^2/(4\pi\epsilon_0 b k_B T_d), \tag{1}$$

where b is the interparticle spacing. For a one-component plasma, strong coupling occurs for $\Gamma>1$, although this criterion does not apply strictly for a dusty plasma, since dust charges are screened by the surrounding ions and electrons. To help correct for this, a common empirical substitute for the coupling parameter is $\Gamma_s=\Gamma\exp(-b/\lambda_D)$. For many laboratory experiments Γ_s cannot be calculated accurately because often neither λ_D (in a plasma with $T_e\neq T_i$ and drift-

[a]Present address: Applied Materials, 3100 Bowers Ave., Santa Clara, California 95054.
[b]Author to whom correspondence should be addressed; electronic mail:

 1070-664X/96/3(4)/1212/8/$10.00

ing ions) nor the particle spacing b of small grains is known accurately, and the exponential magnifies these uncertainties.

The literature for wave dispersion and damping in strongly coupled plasmas is sparse compared to that of weakly collisional plasmas, and to the authors' knowledge it does not include any paper specific to dusty plasmas. For electron–ion plasmas there have been several simulations and theories of acoustic waves. For one, Atrazhev and Iakubov[17] recently investigated ion sound propagation and damping in a plasma with $\Gamma > 10$, and noted that the sound velocity and viscous damping increased with Γ. Other papers cited in Ref. 17 reported simulations for lower values of Γ. Some of these references assume quantum-mechanically degenerate electrons,[18] which are not present in our experiments.

In this paper, we report experimental observations of very low-frequency macroscopic modes in a laboratory dusty plasma. The phase velocity we observe is comparable to the dust thermal speed, which is suggestive of a sound or acoustic wave. The mode might also be an ionization wave. We draw attention to the lack of suitable theories, including a theory of dust acoustic waves that is valid in strongly coupled dusty plasmas and a theory for ionization waves in dusty plasmas.

II. EXPERIMENTAL PROCEDURE

Here we describe briefly the experimental apparatus and procedure. Other details can be found in Ref. 19, which reports data from the same experiment as for this paper. In the present paper we deal mainly with wave phenomena with a short time scale, whereas Ref. 19 describes the dust cloud's evolution over a long time scale.

A radio-frequency discharge was formed between parallel-plate electrodes, as shown schematically in Fig. 1. The electrodes were 6.2 cm diam and separated by 2 cm. They were covered with graphite targets, which were sputtered by ions during the experiment. The resulting carbon atom vapor nucleated in the gas phase, producing nanometer size particulates that continued to grow by accretion of carbon atoms onto their surfaces. The lower electrode was grounded, while the upper was powered by a radio-frequency generator. The generator was coupled to the electrode through an impedance-matching network and a coupling capacitor. A power of 110 W was applied, developing a dc self-bias of -470 V. The frequency of 13.56 MHz was high enough that only the electrons could respond. Ions and dust particles move only in response to dc or very low-frequency fields. Argon flowed through the chamber at a constant rate of 157 sccm to maintain a 55 Pa pressure. At this pressure, the plasma had a fractional ionization of about 10^{-6}. The neutral gas damps the motion of the particulates with an exponential decay time on the order of milliseconds, computed using the Epstein drag law.

In this experiment the particulates, too small to be imaged individually, were seen as a cloud. To record images, a sheet of laser light was formed by passing an argon–ion laser beam ($\lambda_{laser} = 488$ nm) through a cylindrical lens to illuminate a vertical plane in the vacuum vessel. A video camera focused on this plane, with the camera viewing at 45° from the

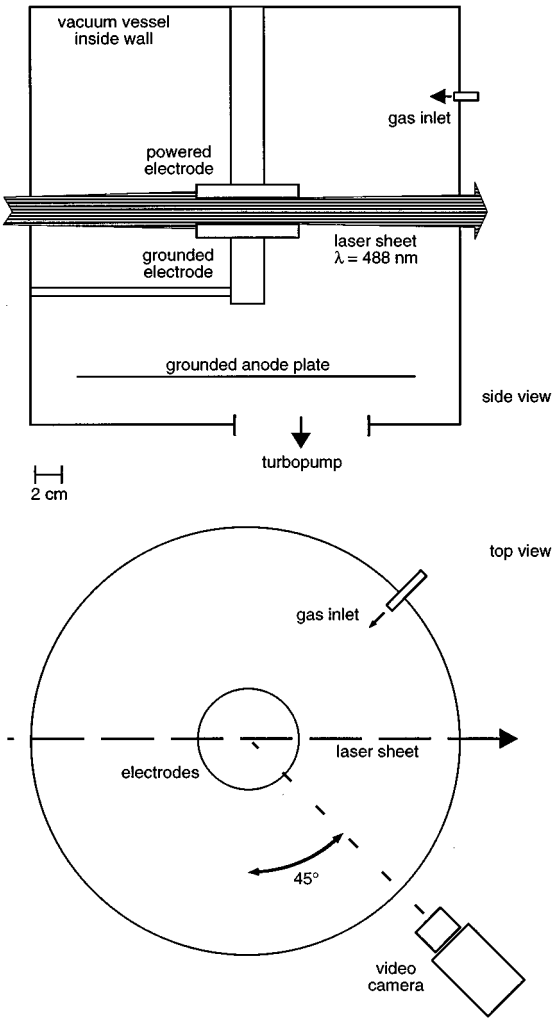

FIG. 1. Sketch of the apparatus. The plasma was formed between two parallel-plate circular electrodes. A cloud of carbon particles that grew in the plasma was illuminated by a laser sheet and imaged at 45° by a video camera.

forward direction. Because of this viewing angle, images appear to be compressed by a factor $1/\sqrt{2}$ in the horizontal direction. The camera operated at 30 frames per second, and it was fitted with a bandpass interference filter to block the plasma glow. Video frames were digitized with eight bits of intensity resolution and recorded on a computer, where the images presented here, such as Fig. 2, were produced. This method of video imaging provided data that are more informative and visual than the single-point measurements we recorded in a previous experiment.[3]

Dust grains were synthesized in the plasma during the discharge operation. They were charged and levitated between the electrodes, where they were exposed to the carbon flux. In a test, we found no measurable extinction of the laser light in a single pass through the dust cloud, indicating that it was optically thin.

We estimate that the grain number density in our experiment lay between a lower bound of 3×10^{3} cm^{-3} and an upper bound of 1.7×10^{7} cm^{-3}. The lower bound was estimated from our observation that we achieved an easily detectable signal[20] and the upper bound comes from our finding

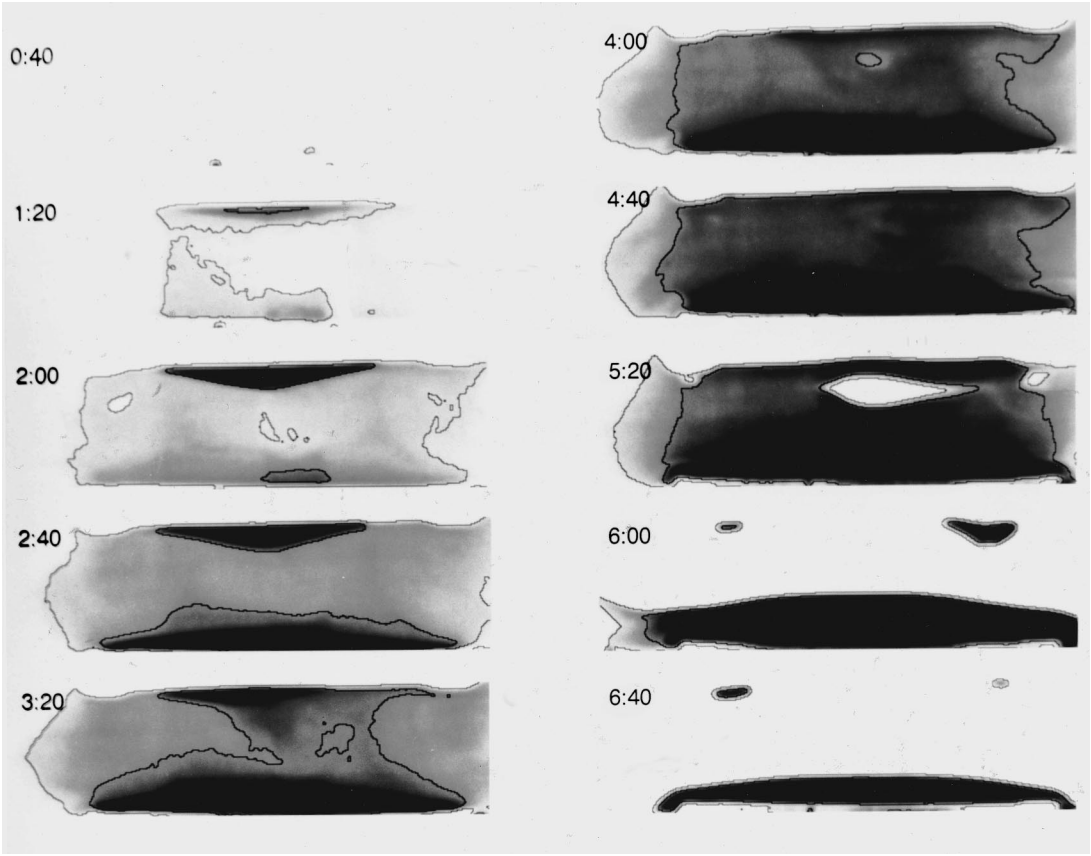

FIG. 2. Images of the first cycle of growth. Time is denoted in (mm:ss), beginning when the plasma was turned on. The height of the image is 2 cm, showing the full interelectrode spacing, while in the horizontal direction appears compressed by a factor $1/\sqrt{2}$ due to the camera's viewing angle. In this 256-level gray scale, black denotes the strongest intensity. The solid lines are contours at intensity levels 20 and 125, to aid the eye in identifying features at low intensities.

that the dust cloud was optically thin. In making these estimates, we used a Mie scattering code[21] to compute scattering and extinction rates, and we assumed spherical particles with a complex refractive index of $(2-i)$. This range of densities is wide, but it is sufficiently accurate for the purpose we use below in comparing the observed phase velocity to the value predicted by a wave dispersion theory.

In separate tests that were carried out with the same operating parameters, we terminated the discharge after various exposure times. The lower electrode, where many of the particles landed, was transferred to a scanning electron microscope (SEM), producing micrographs that are presented elsewhere.[4,22] After 10 min of plasma exposure, the SEM images showed that the particles were uncoagulated spheroids with a diameter of (154 ± 10) nm. After 20 min, the diameter of the spheroids had doubled, indicating a linear growth rate of about 15 nm/min. The ±10 nm diam range is the one-sigma level of the size dispersion. It corresponds to a $\pm6\%$ dispersion, which is narrower than in some other wave experiments.[13]

With a growth rate of 15 nm/min, the particles were smaller than 0.2 λ_{laser} during the first 6 min of operation. Thus, the images of the dust cloud were due to Rayleigh scattering, with a scattered intensity proportional to the sixth power of the particle size and the first power of the dust number density. The brightness in our images, therefore, is a function of both the size and density. Over the course of tens of seconds, the images become noticeably brighter overall because the particles are growing in size. On the shorter time scale of the modes we report below (typically 0.1 s) the brightness fluctuates; this is attributed to a compression and rarefaction of the dust cloud. An alternate explanation would be a fluctuating segregation of smaller and larger particles to different regions of the discharge, but this seems unlikely since the particle dispersion is narrow.

A time series of the brightness shown in Fig. 3 was prepared from segments of the video. This was done by averaging the gray-scale values over a square region of 8×8 pixels, corresponding to a few square mm, located halfway between the electrodes in the vertical direction and halfway between the center and the edge of the electrodes in the horizontal direction. The memory available in our video digitization equipment limited us to recording a time series for 32 consecutive video frames.

III. RESULTS

The particulates grew to a visible size and density after less than a minute. They formed a cloud that filled the interelectrode region and then collapsed. The growth and collapse process repeated in a 7 min cycle. During the growth process, some particles flowed out of the cloud and were lost, while others were retained for up to several hours, growing to a size of several microns. New particles were constantly

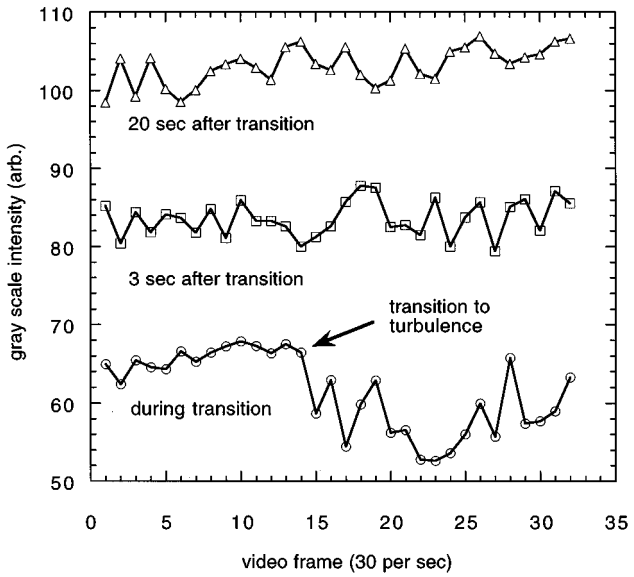

FIG. 3. Time series of laser scattering intensity during the filamentary mode. The gray scale intensity was averaged over a small square region located halfway between the electrodes in the vertical direction and halfway between the center and the left edge of the electrodes in the horizontal direction. Note the sudden transition to turbulence and the subsequent spectrum of low frequencies. Between the three segments shown here there was a secular increase in scattering intensity due to growth in the particle diameter.

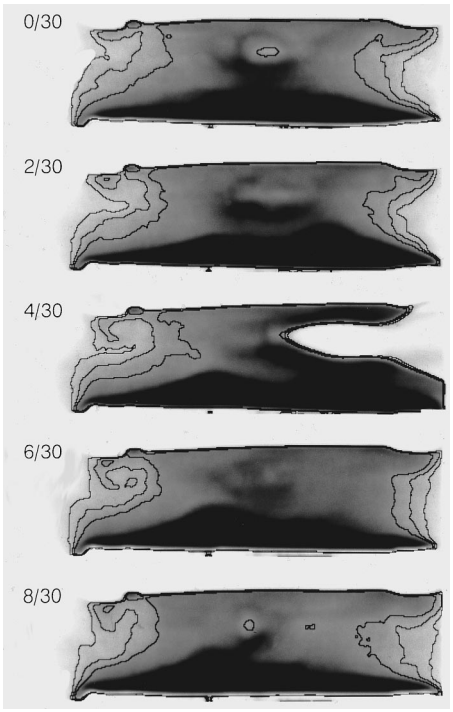

FIG. 4. Filamentary mode. Images shown here are every other video frame, which were recorded at 30 frames per second. Both the filament and great void modes were active at the stage shown here. One feature of the filament mode is a vortex, which is seen rolling in the counterclockwise direction in the upper left side of these images. In the video, stimulation of the vortex appeared to be synchronized with the orbit of the great void, which executed a full circular orbit, with a period longer than in Fig. 5. The void is seen here only in frame 4/30. Filamentary modes also can be seen in the central cloud region. Every other frame is shown here, for images recorded at $t=8{:}39$. The solid lines are contours at intensity levels 100, 120, and 140.

created during the plasma operation. Other experimenters have also observed periodic cloud growth and collapse.[23,24] In this paper we will emphasize the mode behavior exhibited during the first 1.5 cycles, which are typical of the later cycles as well.

The first cycle is shown in Fig. 2. The images have been cropped to show only the full 2 cm high interelectrode spacing. In the early stages, the entire interelectrode region was filled with particles, with a higher concentration in an inverted dome near the upper electrode, where the source of sputtered carbon atoms was most intense. Initially the dust cloud evolved smoothly and quietly. There was a small ring-shaped void (width 3 mm, diameter 1.2 mm), which appears white in the image. Additional images of the first cycle are reported in Ref. 16.

As seen in Fig. 3, the cloud suddenly became turbulent at $t=1{:}53$. (Time is given here in min:s, beginning when the plasma was switched on.) In the video the turbulence was manifested as oscillating filamentary structures. They were present in a large portion of the interelectrode region, and at first they were especially pronounced in the region where the small void was. The turbulent state ended later at $t=5{:}45$, just as abruptly as it began. This cessation of turbulence coincides with the splitting in two of the dust clouds.

The filamentary mode persisted during the entire turbulent period (from $t=1{:}53$ to 5:45). It had the appearance of striations, which are visible in Fig. 2 in the frames at $t=4{:}00$ and 4:40. They are seen more easily in the moving video than in these still images. From the time series shown in Fig. 3, we estimate that the filamentary mode had a frequency spectrum ranging from about 5 Hz to at least the Nyquist frequency of 15 Hz.

After the great void mode developed, the striations in the outer half-diameter region took the form of a distinctive vortex that swirled with a curling motion in the poloidal direction. This appeared on both the left and right sides of the images, although it was sometimes more obvious on the left, as in the images shown in Fig. 4. This vortex appeared immediately behind, i.e., in the wake, of the rotating great void. The frequency for the vortex to curl up to a full 360° winding was about 15 Hz at $t=2{:}04$ when the vortex was 0.4 cm wide in the image plane. Later, the curling slowed to a frequency of 6 Hz at $t=3{:}29$ and 5 Hz at $t=4{:}29$. The frequencies cited above are accurate to about a factor of 2.

The mode we term the great void mode appeared after the filamentary mode developed. The first indications were apparent at about $t=3{:}14$. At that time a large oscillating structure with a low amplitude formed in the unstable outer half-diameter region. By $t=4{:}10$ it developed into a persistent large spoke-shaped void that rotated in the azimuthal direction with a period of several seconds. The filamentary mode was still present, but now its oscillations appeared to be coupled to the great void, which appears white at $t=5{:}20$ in Fig. 2. Visual observation revealed that the great void was accompanied by a concentrated glow in the plasma that rotated at the same speed. (The glow cannot be seen in the optically filtered video images reported here.) A brighter glow usually indicates that electrons are denser or hotter than

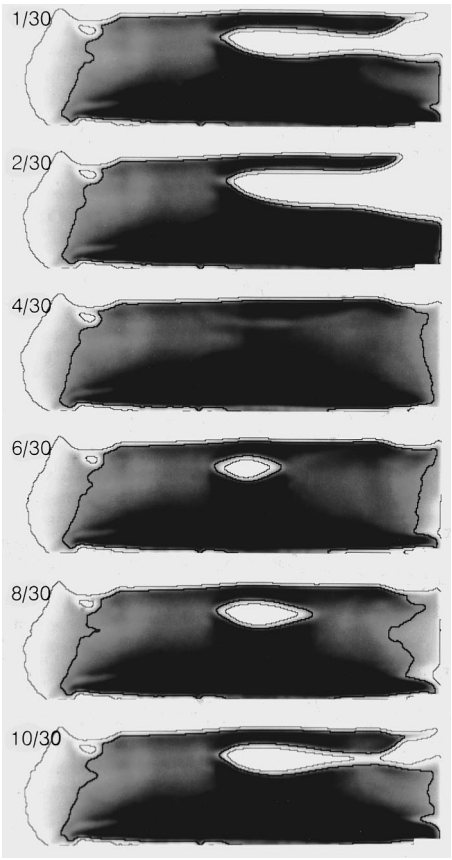

FIG. 5. The great void mode. The void is seen executing a half-circular orbit on the right side of the picture. It appears to have a radial spoke shape. The images at 1/30 s and 10/30 s are almost identical, indicating the period is 9/30 s and the frequency is 3.3 Hz. The small void in the upper left appears undisturbed during the orbit of the great void. Some filamentary structures were present at this time, although they are easier to identify in the moving video than in these still frames. These images were recorded at $t=4{:}50$. The solid lines are contours at intensity levels 20 and 125.

usual. This observation of a moving glow leads us to speculate below that the great void mode may be a kind of ionization wave.

The great void rotated in a horizontal plane, and initially it circled fully around the plasma in the azimuthal direction. Then its orbit ceased to make a full circle, going around only halfway, on the right-hand side (facing the gas inlet), as seen in the sequence of images in Fig. 5. This sequence shows a single orbit of the mode, with an interval of 2/30 s between images. At this time ($t=4{:}50$), the great void rotated with a frequency of (3.3 ± 0.3) Hz. Shortly thereafter it slowed to a halt while facing to the right, the turbulent striations stopped, and the cloud split in two.

After the splitting in half of the cloud at $t=5{:}45$ was an abrupt transition. Afterward, the clouds were quiet, with no filamentary turbulence. Remaining after this event were a ring near the upper electrode and a flattened dome above the lower electrode. The edges of the lower dome hung over the electrode edge, so that the radial particle flow or escape from the interelectrode region was especially pronounced while the cloud was in this collapsed state. At $t=7{:}07$, the lower cloud attained its minimum thickness, marking the end of the first cycle. After that, the second cycle commenced with particles flowing from the lower to the upper cloud, filling the interelectrode region. The cycle repeated with a reliable period many times, until the discharge was shut off.

IV. DISCUSSION

A. Forces on the particles

Dust grains experience electrostatic, drag, and gravitational forces. The electrostatic force must play a role in the modes and instabilities, just as it does in the particle levitation. This force scales linearly with the particle charge, and therefore linearly with the particle size. In equilibrium, it drives particles away from the electrodes and toward the plasma center, where the plasma potential has its maximum. The ion drag force is the momentum transfer from Coulomb collisions with ions flowing toward a grain. This force pushes particles in the direction of ion flow, which, in equilibrium, is toward the electrodes. The gravitational force scales as the third power of the grain size, and it is probably not significant in our experiment, due to the small particle size.

There is also a neutral gas flow, since argon is constantly admitted and evacuated from the vessel. This creates a drag force, which in the molecular flow regime scales with the square of the particle size. The neutral drag perturbs the dust cloud but does not determine the overall vertical levitation of the grains, according to tests we conducted in another vacuum vessel. The gas flow is the only asymmetry in the vacuum vessel, and it therefore probably accounts for the asymmetry we observed in the great void mode, which made its final half-circle orbits and came to a rest always on the upwind side of the cloud, as seen in Fig. 5. It is unlikely, however, that the gas flow is the responsible agent for causing the great void or the filamentary modes. It is difficult to reconcile how gas flow can lead to a transition where the entire quiet dust cloud is suddenly filled with the turbulent filamentary modes. The abrupt and global nature of this transition seems more suggestive of an electric interaction, although we have no detailed theory to predict it. Likewise the great void mode terminates with the vertical collapse of the cloud that occurs simultaneously over the horizontal extent of the electrode. The collapse is certainly linked to the vertical levitation mechanism of the dust, which is due to electrical and ion drag forces, and not the neutral gas flow.

B. Characteristics of the modes

Both the filamentary and great void modes arise due to instabilities that occur in the middle of the cycle. While we are unable to identify exactly the mechanics of the instabilities, we are able to find several clues in the cyclic nature of the cloud growth and collapse. The overall shape of the cloud is determined by an equilibrium balance of the electric and drag forces. Since these forces scale differently with particle size, and the particle size grows with time, it is to be expected that the equilibrium cloud shape will evolve over time. The splitting and collapse of the cloud near the end of a cycle are part of the evolution of the equilibrium. The fact that the splitting of the cloud not only marks the end of the great void mode, but also coincides with the cessation of the

filamentary turbulence, suggests that the force balance that provides the vertical levitation of the cloud furnishes somehow the free energy that drives these modes. The great void mode serves the important role of being the vehicle that can saturate by splitting the dust cloud in half, as the changing equilibrium due to growing particle size requires. After the splitting the cycle can be completed without any mode activity. The radial loss of particles from the dust cloud empties the cloud enough for the original equilibrium to return.

The very low-frequency and phase velocity of the modes we observed and the lack of an applied magnetic field exclude many familiar plasma waves and instabilities as candidates for explaining our observations. We estimate that our ion density was about 5×10^{10} cm^{-3}, based on measurements made in similar apparatus by other experimenters.[25] This corresponds to an ion plasma frequency of 7 MHz. Ion acoustic waves would range from this frequency downward to about 10^5 Hz, far higher than our observations.

We also can exclude any effects that depend on the finite charging time τ of the grains. Like a capacitor, a grain holds a charge, which can be changed over a finite τ. For our experiment, we computed[2] that $\tau\approx20$ μs for 100 nm diam grains, which is much too fast to alter the very low-frequency modes we observed.

The phase velocity $v_\phi=f\lambda$ can be estimated from the experimental data by approximating the wavelength λ with the scale length we see in the images. The vortices we saw in the filamentary mode swirled in a full poloidal rotation with a frequency $f=15$ Hz, and had a transverse scale length of 0.4 cm. These values are for images taken during the first cycle, at $t=2{:}04$. The great void mode had $f=1.5$ Hz and a transverse width of 4 cm, at $t=5{:}29$. These values yield a phase velocity $v_\phi\approx6$ cm/s that is the same for the two modes, accurate within a factor of 4.

The filamentary mode usually had a low amplitude. In its manifestation as a vortex, it registered as a perturbation of only several levels on our 256-level video digitizer. It may be possible to explain this as a linear or weakly nonlinear mode. The amplitude of the great void, on the other hand, spanned the entire dynamic range of the digitizer, suggesting that it is nonlinear.

C. Identifying the modes

Here we discuss two possible explanations for our modes: a dust-acoustic wave and a dust-mediated ionization wave. The dust-acoustic wave is a compressional sound wave, with a phase velocity comparable to the dust thermal speed. An ionization wave is a disturbance in the balance of the source and loss of plasma.

1. Dust-acoustic wave

The dispersion relation of the dust-acoustic mode has been derived from a Vlasov model by Melandsø *et al.*[26] and by D'Angelo[12] using a two-fluid model of the plasma. These are both suitable for weakly coupled plasmas. Both also assume low-amplitude linear perturbations. The expressions in these two papers differ slightly due to different manners of accounting for the electron space charge depletion at high dust number densities and other minor differences, but the main features are the same. They have the general form $(\omega/k)\approx[(k_\mathrm{B}T_d/m_d)+\omega_{pd}^2\lambda_\mathrm{D}^2]^{1/2}$, which is nondispersive, assuming $k\lambda_\mathrm{D}\ll1$, which is suitable for the large wavelengths present in our experiment. We assume single-size dust grains with a temperature T_d, mass m_d, charge number $Z=Q_d/e$, number density n_d, dust plasma frequency $\omega_{pd}=(n_dQ_d^2/\epsilon_0m_d)^{1/2}$, and λ_D is the total Debye length due to both the electrons and ions. The wave will propagate only if $\omega/k\gg(k_\mathrm{B}T_d/m_d)^{1/2}$, to avoid Landau damping on the ions,[26] so that the phase velocity is nearly equal to the dust acoustic speed, $\omega_{pd}\lambda_\mathrm{D}$. Another collisionless damping mechanism proposed by Melandsø *et al.*,[26] due to the finite charging time of the grains, has little effect in our experiment due to the large discrepancy between the charging time and the observed wave period. D'Angelo's expression for the dispersion relation can be written as

$$\frac{\omega}{k}=\left(\frac{k_\mathrm{B}T_d}{m_d}\right)^{1/2}\left(1+\frac{T_i}{T_d}\,\epsilon Z_d^2\,\frac{1}{1+(T_i/T_e)(1-\epsilon Z_d)}\right)^{1/2}, \tag{2}$$

where $\epsilon=n_d/n_i$. In a gas discharge, the factor T_i/T_d in Eq. (2) is nearly unity. For our experiment, we estimate using a standard charging model[2] that our 100 nm diam particles had a charge $Z_d\approx200$. The final quotient appearing on the right-hand side of Eq. (2) is of order unity, since $T_i\ll T_e$ in a gas discharge. Using the upper and lower bounds on the dust number density in our experiment, the factor ϵZ_d^2 lay in the range $10^{-3}<\epsilon Z_d^2<140$. Thus, the phase velocity lies in a range from 1 to 12 times the dust thermal velocity, $1\leqslant[(\omega/k)/(k_\mathrm{B}T_d/m_d)^{1/2}]<12$. At the lower end of this range the wave would not propagate due to ion Landau damping, while at the middle to the upper end of the range propagation would be possible.

The dust thermal speed $(k_\mathrm{B}T_d/m_d)^{1/2}$ in our experiment is estimated to be 6 cm/s at the end of the first cycle. This assumes 100 nm diam particles of mass density 2.2 g/cm^3 and kinetic temperature 300 K. The latter value is based on measurements reported by other experimenters.[27] One should bear in mind that the thermal speed is proportional to the diameter to the $-\frac{3}{2}$ power, and the particles grew in diameter at a rate of 15 nm/min in our experiment. Thus, the thermal speed diminished by a factor of 2 over the time span the phase velocity measurements listed above.

The experimentally measured phase velocity of 6 cm/s (accurate to a factor of about 4) is comparable to the estimated phase velocity. The latter is a multiple of one to 12 times the thermal velocity of 6 cm/s. This comparison should not be overemphasized, however, because Eq. (2) was derived for a linear perturbation in a weakly coupled plasma. Our dust may have been strongly coupled and the great void was definitely nonlinear.

2. Ionization wave

The glow in the plasma was strongly modulated when the great void mode was active. In the experiment we saw that the glow was enhanced profoundly in a localized region that rotated synchronously with the void in the dust cloud. Glow in a gas discharge is produced by electron-impact ex-

citation of neutrals by the same fast electrons that produce ionization. The modulation in the glow indicates that the nonlinear dust void was linked to a time-varying fast electron component. Other experimenters using a gas discharge have not reported such a modulation in the glow, although the possibility cannot be ruled out since their apparatus may not have allowed it to be seen as clearly as in ours.[13] Similarly, we did not see a glow variation corresponding to the striation mode, although the much lower amplitude of the striation mode may have made any such variation undetectable to the unaided eye.

These visual observations indicate that the great void mode is something more than an acoustic wave. Electron energetics certainly play a role. This brings us to search for a mechanism involving ionization that might be at work.

One type of mode that can be sustained in a nondusty gaseous discharge is an ionization wave.[28] This disturbance, which is familiar in glass discharge tubes such as old fluorescent light bulbs, is visible to the eye. There are a wide class of these modes, which are produced by a disturbance in the balance of ionization (which is linked to the electron energetics) and plasma loss. Those with the lowest frequency appear as a stationary or moving striation in the glow with such a low frequency and long wavelength that they are visible to the eye. In one common form, a slight increase in electron temperature causes an enhanced ionization of metastable neutrals, augmenting the electron density until a relaxation in the ionization rate diminishes the electron density and the cycle repeats. The electron temperature and electron density are often not in phase. The class of modes termed relaxation oscillations typically have a frequency of $10–10^4$ Hz and a large amplitude. They are dependent on the external circuit and the diameter of the glass surface, where plasma is lost.[28]

In a dusty plasma, the surface recombination would, in effect, be distributed throughout a cloud of dust in the plasma. Local electric fields might be generated in nonneutral boundaries between the dusty and clean plasma regions, and these would tend to push the dust cloud around. The electron temperature is believed to increase with dust density, leading to a higher ionization rate.[29] Thus, a moving dust cloud of the type we observed would cause a propagating temperature and ionization wave. We are therefore led to speculate that such an ionization wave may be responsible for the great void mode. However, a quantitative theoretical analysis is required to draw a firm conclusion. To the authors' knowledge, no such theory has been developed in the literature.

D. Waves in strongly-coupled dusty plasmas

Here we draw attention to a significant shortcoming in the state of theory for waves in dusty plasmas. While the electrons and ions in a laboratory dusty plasma are weakly collisional among themselves, the charged grains often are not. They are strongly coupled, meaning that they are dominated by Coulomb collisions between neighboring particles. One measure of this is the ordered structure that can be seen when the individual grains are imaged in plasma crystal experiments.[5–11] Another measure is the Coulomb-coupling parameter, defined in Eq. (1).

Chu and I[7] reported very low-frequency ($\approx$12 Hz) modes with a wavelength of about 0.5 cm. Their particles had a diameter of 10 μm, and accurate video imaging showed an ordered structure with a spacing of about 0.3 mm. We estimate that the Coulomb coupling parameter was $\Gamma \approx 8\times 10^4$ in their experiment, assuming $T_d = 0.025$ eV, $T_e = 2$ eV, and $T_i = 0.05$ eV. This estimate neglects the effects of the ion drift speed and the dimensionless dust number density P (defined in Ref. 2), factors that might alter the charge by 30%. It also neglects screening effects. Regardless of the calculation of Γ, however, it is certain that the plasma was strongly coupled, since video images of the grains showed that they formed an ordered structure similar to a Coulomb lattice.

In our experiment the particles were smaller by a factor of 10^{-2} compared to those of Chu and I. For this reason our particles could not be imaged individually to reveal any order that might be present. It also means that the coupling was weaker in our experiment. Noting that Γ scales as the square of the charge and that the charge is proportional to particle size, this means that Γ would be smaller by a factor of 10^{-4} in our experiment if the interparticle spacing and other parameters were the same. In fact, the particle spacing in our experiment was surely less, and the coupling was therefore probably not reduced by such a large factor. It is thus likely that $\Gamma > 1$ in our experiment, but we cannot say whether Γ_s was greater or less than unity. We cannot state definitely whether our dust grains were strongly or weakly coupled because of the impracticality of structural imaging and accurate measurement of particle spacing. Our measurements centered instead on the dynamics of the dust cloud.

V. CONCLUSION

We have reported laboratory observations revealing macroscopic very low-frequency modes of a charged dust cloud in a gaseous discharge. The filamentary mode was a striation, and it sometimes had a distinctive vortex appearance. The other, which we term the great void mode, was a rotating region lacking any detectable dust. These modes had frequencies in the range 1 to 15 Hz, and a phase velocity of typically 6 cm/s. They might be explained either as dust-acoustic modes or dust-mediated ionization waves. There is a need for better developed theories for these modes, including strongly coupling effects in a dusty plasma. After we submitted this paper and shared a preprint of it with Wang and Bhattacharjee, they developed a kinetic theory for very strongly coupled dusty plasmas, which may be useful for dust-acoustic waves.[30] No theory has yet been developed for dust-mediated ionization waves, to the authors' knowledge.

ACKNOWLEDGMENTS

The authors thank F. Melandsø, R. Merlino, A. Bhattacharjee, and the participants of the 1995 Dusty Plasma Workshop in Wickenburg Arizona for helpful discussions.

This work was supported by the National Science Foundation (Grant No. ECS-92-15882) and the National Aeronautics and Space Administration (Origins of the Solar System Program Grant No. NAGW-3126 and Microgravity Science and Applications Division Grant No. NAG8-292).

[1]C. K. Goertz, Rev. Geophys. **27**, 271 (1989).
[2]J. Goree, Plasma Sources Sci. Technol. **3**, 400 (1994); and J. Goree, ''Charge on dust grains with a finite number density in a plasma,'' to appear in IEEE Trans. Plasma Sci.
[3]G. Praburam and J. Goree, J. Vac. Sci. Technol. A **12**, 3137 (1994).
[4]G. Praburam and J. Goree, Astrophys. J. **441**, 830 (1995).
[5]H. Thomas, G. Morfill, V. Demmel, J. Goree, B. Feuerbacher, and D. Möhlmann, Phys. Rev. Lett. **72**, 652 (1994).
[6]J. H. Chu, J. B. Du, and L. I, Phys. Rev. Lett. **72**, 4009 (1994).
[7]J. H. Chu and L. I, J. Phys. D **27**, 296 (1994).
[8]Y. Hayashi and K. Tachibana, Jpn. J. Appl. Phys. **33**, L804 (1994).
[9]A. Melzer, T. Trottenberg, and A. Piel, Phys. Lett. A **191**, 301 (1994).
[10]T. Trottenberg, A. Melzer, and A. Piel, Plasma Sources Sci. Technol. **4**, 450 (1995).
[11]R. Quinn, J. Goree, C. Cui, H. Thomas, and G. Morfill, ''Structural analysis of plasma crystal experiments,'' to appear in Phys. Rev. E.
[12]N. D'Angelo, J. Phys. D Appl. Phys. **28**, 1009 (1995).
[13]A. Barkan, N. D'Angelo, and R. E. Merlino, Phys. Plasmas **2**, 3563 (1995).
[14]N. N. Rao, P. K. Shukla, and M. Y. Yu, Planet. Space Sci. **38**, 543 (1990).
[15]F. Melandsø, T. Aslaksen, and O. Havnes, Planet. Space Sci. **41**, 321 (1993).
[16]P. K. Shukla, Phys. Scr. **45**, 507 (1992) and other papers in the same issue.
[17]V. M. Atrazhev and I. T. Iakubov, Phys. Plasmas **2**, 2624 (1995).
[18]M. A. Berkovsky, Phys. Scr. **51**, 769 (1995).
[19]G. Praburam and J. Goree, ''Evolution of a particulate cloud in an RF plasma,'' to appear in IEEE Trans. Plasma Sci.
[20]G. Praburam and J. Goree, ''Sensitivity of the scattering ratio method for sizing submicron particles suspended in a plasma,'' to appear in Plasma Sources Sci. Technol.
[21]C. F. Bohren and D. R. Huffman, *Absorption and Scattering of Light by Small Particles* (Wiley, New York, 1983).
[22]G. Praburam and J. Goree, ''Plasma method of synthesizing aerosol particles,'' to appear in J. Aerosol Sci.
[23]C.-K. Yeon and K.-Whang, J. Vac. Sci. Technol. A **13**, 2044 (1995).
[24]E. Stoffels, W. W. Stoffels, G. M. W. Kroesen, and F. J. de Hoog, ''Dust formation and charging in an Ar/SiH_4 radio-frequency discharge,'' to appear in J. Vac. Sci. Technol.
[25]L. J. Overzet, J. Res. Nat. Inst. Standards Technol. **100**, 401 (1995).
[26]F. Melandsø, T. K. Aslaksen, and O. Havnes, J. Geophys. Res. A **98**, 13 315 (1993).
[27]L. Boufendi, A. Bouchoule, R. K. Porteous, J. Ph. Blondeau, A. Plain, and C. Laure, J. Appl. Phys. **73**, 2160 (1993).
[28]A. Garscadden, in *Gaseous Electronics Vol. I, Electrical Discharges*, edited by M. N. Hirsch and H. J. Oskam (Academic, New York, 1978), p. 65.
[29]J. P. Boeuf, Phys. Rev. A **46**, 7910 (1992).
[30]X. Wang and A. Bhattacharjee, Phys. Plasmas **3**, 1189 (1996).